Processing and Application of Ceramics 15 [3] (2021) 238–245
https://doi.org/10.2298/PAC2103238K

Effect of PEG-based binder concentration on the mechanical properties of lithium disilicate glass-ceramics prepared by low-pressure injection moulding

Arnon Kraipok[1,2], Pratthana Intawin[3], Manlika Kamnoy[1], Suchittra Inthong[4], Wilaiwan Leenakul[5], Patamas Bintachitt[6], Sukum Eitssayeam[1], Orawan Khamman[1], Tawee Tunkasiri[1], Kamonpan Pengpat[1,*]

[1]*Department of Physics and Materials Science, Faculty of Science, Chiang Mai University, Chiang Mai 50200, Thailand*
[2]*Graduate School, Chiang Mai University, Chiang Mai 50200, Thailand*
[3]*Division of Physics, Faculty of Science and Technology, Rajamangala University of Technology Thanyaburi, Pathum Thani, 12110, Thailand*
[4]*Faculty of Agricultural Science and Technology, Rajamangala University of Technology Lanna Phitsanulok, Phitsanulok, 65000, Thailand*
[5]*Division of Industrial Materials Science, Faculty of Science and Technology, Rajamangala University of Technology Phra Nakhon, Bangkok 10800, Thailand*
[6]*Department of Physics, Faculty of Science, Srinakharinwirot University, Bangkok 10110, Thailand*

Received 14 December 2020; Received in revised form 14 April 2021; Accepted 16 July 2021

Abstract

Lithium disilicate (LD) glass-ceramics are extensively employed in restorative dentistry because their superior aesthetic properties and hardness are similar to natural teeth. The aim of this work is to investigate the mechanical properties and chemical solubility of lithium disilicate glass-ceramics prepared by the low-pressure injection moulding using the PEG-based binder. The glass-to-binder ratio was varied as 60:40, 55:45, 50:50 and 45:55 vol.%. The sintering conditions of 800 °C with 2 h dwell time were selected according to thermal analysis. Phase formation, microstructure and mechanical properties of the prepared samples were characterized by XRD, SEM, microhardness and three-point bending test, respectively. Besides, the chemical solubility of the system was investigated by the immersion test in acetic acid solution. XRD analyses of the sintered sample confirmed the presence of only one prominent crystalline phase of LD. SEM result showed that the porosity increased with decreasing glass powder content. The mechanical properties of the LD glass-ceramic samples tended to decrease when the proportion of the glass powder decreased, while the chemical solubility tended to increase. The mechanical properties of the glass-ceramics, i.e. the highest density value, Vickers hardness and flexural strength were 2.55 g/cm^3, 6.80 GPa, and 176 MPa, respectively. These results could be useful in developing these LD glass-ceramics for their optimal use in dental applications.

Keywords: *lithium disilicate, injection moulding, mechanical properties, dental materials*

I. Introduction

Lithium disilicate (LD) glass-ceramics have been extensively employed in restorative dentistry such as implants, crowns and bridges due to their excellent biocompatibility, chemical durability, similar hardness to teeth and translucency, as well as very high fracture strength and adequate fracture toughness [1,2]. These properties result from the high-volume fraction of elongated micron-sized LD crystals and some minor phases, which form an interlocking network embedded into a residual glass [3]. The properties of LD glass-ceramics

*Corresponding author: tel: +66 53 943 376,
e-mail: *kamonpan.p@cmu.ac.th*

can also be modified by varying the composition of the glass or controlling the heat treatment process [4–6]. These glass-ceramics are obtained from glasses of the SiO_2-Li_2O system, containing some additive oxides such as nucleating agent (P_2O_5), glass modifiers (K_2O) and glass intermediates (Al_2O_3 and CaO) [7–10]. The previous work showed that the increase of P_2O_5 content reduces the crystallization temperature and increases nucleation density [11]. Furthermore, the maximum fracture strength of the LD glass-ceramics with 1 mol% P_2O_5 content could reach 310 MPa, as reported by Wang *et al.* [12]. Moreover, Fernandes *et al.* [13] found that the small addition of Al_2O_3 and K_2O to the pure Li_2O-SiO_2 system enhanced the densification behaviour and the ultimate mechanical strength. The coloured shades of these glass-ceramics could be improved by adding some oxides such as CeO_2, Fe_2O_3, MnO_2, V_2O_5 and TiO_2 in the parent glass compositions [14,15].

Ceramic injection moulding (CIM) is normally used to produce complex-shaped components from feedstock composed of ceramic powders with thermosetting or thermoplastic binders, which render the required fluidity level of powder/binder mixture for successful injection moulding [16]. CIM has two principal methods consisting of high-pressure injection moulding (HIM) and low-pressure injection moulding (LIM) [17]. The advantages of LIM over HIM process are lower costs, shorter binding time, more moderate die wear and the recycling ability of slip remainders [17]. The proper use of binders is crucially important in the processing method of this CIM technique. The binder system consisting of polyethylene glycol (PEG), polyvinyl butyryl (PVB) and stearic acid (SA) is used to improve the flow characteristics of the LD feedstock [18]. PEG is a very safe chemical and it is used extensively in the food industry, and PVB facilitates excellent wetting characteristics with powder and provides homogeneous feedstock [19]. At the same time, SA is used as a lubricant to make the mixture ready to combine with increasing the strength of the binder [20].

Therefore, this study has been concentrated on the mechanical properties and chemical solubility in the low-pressure injection moulding of the LD glass-ceramics using PEG-based binder for dental material application. The LD glass-ceramics were prepared using Li_2O-SiO_2-P_2O_5-Al_2O_3-K_2O-CaO as the base glass system by the conventional melt quenching method. The binder system used in this study consisted of PEG, SA and PVB, mixed with glass powder with the glass-to-binder ratio of 60:40, 55:45, 50:50 and 45:55 vol.%. The thermal properties, phase formation and microstructure of the samples were investigated by differential thermal analysis (DTA), X-ray diffractometer (XRD) and scanning electron microscope (SEM), respectively. Bulk density, linear shrinkage, porosity, Vickers hardness, Knoop hardness, Young's modulus, fracture toughness and flexural strength results were used to analyse the mechanical properties of the samples. Also, the chemical solubility of the prepared glass-ceramics was evaluated by the immersion test in acetic acid solution.

II. Experimental

Glass preparation: The LD glass with the composition of 15.64 Li_2O, 69.20 SiO_2, 3.37 P_2O_5, 3.54 Al_2O_3, 3.25 K_2O and 5.00 CaO (mol%) was prepared using the conventional melt quenching method. The raw materials of the glass consisted of Li_2CO_3, SiO_2, $(NH_4)_2HPO_4$, Al_2O_3, K_2CO_3 and $CaCO_3$ with analytical grades and purity of more than 99.0% (Sigma-Aldrich, Singapore). These raw materials were mixed and melted in an alumina crucible at 1450 °C for 2 h in a high-temperature furnace in an air atmosphere with a heating rate of 10 °C/min and quenched in distilled water at room temperature to obtain glass frits. The glass frits were dried in an oven at 150 °C for 4 h, ground in an agate mortar and sieved with a stainless steel sieving mesh (325 mesh size) to achieve glass powder.

Binder preparation: The binder system consisted of PEG (Sigma-Aldrich, Singapore), PVB (Sigma-Aldrich, Singapore) and SA with the purity of more than 98% (PanReac AppliChem and the ITW Reagents, USA), with the ratio of PEG : PVB : SA was 65:30:5 (vol.%) [18]. The PEG, PVB and SA were mixed in a beaker using a magnetic stirrer (IKA, C-MAG HS 7) at 180 °C for 2 h and then the well-mixed solution was cooled down to room temperature. Finally, the binder was cut into small pieces by granulator (ZERMA, GSL 180).

Feedstock preparation: The glass powder and the prepared binder were used to prepare feedstocks with various compositions with glass powder varying from 60 to 45 vol.%. The mixtures were mixed in a beaker with a magnetic stirrer at 180 °C for 30 min, then cooled down to room temperature and finally crushed using the granulator to obtain feedstock granules.

Injection moulding method: The feedstock granules were injected into the mould by the low-pressure injection moulding machine (TJIRIS, AX-YDA) at 120 °C. After that, the green bodies were de-bound by water leaching to remove the PEG for 6 h and thermal pyrolysis to remove residual binders at 500 °C for 2 h. Finally, the green bodies were sintered at the optimum temperature for 2 h with a heating rate of 10 °C/min according to the DTA result to form LD glass-ceramics for dental material applications.

Differential thermal analysis (DTA: 1600 DTA, Du Pont Instrument) was used to analyse the thermal properties of the glass powders for determination of glass transition temperatures (T_g), crystallization temperatures (T_C) and melting temperatures (T_m) in small alumina crucible by using highly pure alumina powder as reference material by heating from room temperature to 1200 °C with a heating rate of 10 °C/min.

Phase formation of the LD glass-ceramic samples

was determined by the X-ray diffractometer (Rigaku, SmartLab) using Cu Kα radiation generated at 30 mA and 45 kV in the 2θ range from 10–60° at a scanning speed of 1 °/min.

The microstructure was examined by the scanning electron microscope (JEOL, JSM-IT300LV). After sintering, the LD glass-ceramic samples were polished and etched by immersion in the 3 wt.% hydrofluoric acid (HF) for 30 s. The glass-ceramic samples were then cleaned with distilled water and coated with gold by ion sputtering device (JEOL, JFC-1200) for 30 s.

The bulk density measurements were conducted on the glass-ceramic samples using the Archimedes' principle, on an analytical balance with an attached density kit. The bulk density of the glass-ceramic samples (ρ) was obtained by the following equation:

$$\rho = \frac{M_{dry}}{M_{dry} - M_{wet}} \rho_{liquid} \tag{1}$$

where, M_{dry} and M_{wet} are the masses of the glass-ceramic samples in air and liquid, respectively, and ρ_{liquid} is the density of water at room temperature.

The linear shrinkage of the glass-ceramic samples (S_L) was calculated using the standard equation:

$$S_L = \left(1 - \frac{l}{l_0}\right) \times 100 \tag{2}$$

where, l_0 and l are the diameter of the glass-ceramic samples before and after sintering, respectively.

The porosity (Po) of the glass-ceramic samples was obtained by employing the following equation:

$$Po = \frac{m_2 - m_1}{m_2 - m_3} \times 100 \tag{3}$$

where, m)1, m_2 and m_3 are the masses of the glass-ceramic samples weighed after drying, in air and in liquid, respectively.

The hardness was measured on a polished surface of the glass-ceramic samples using Vickers and Knoop microhardness measurement (Buehler, Karl Frank GMBH Type-38505) by applying a load of 1 kg for 15 s. The Vickers hardness (HV) was calculated using the standard equation [21]:

$$HV = \frac{1.8544 \cdot P}{d^2} \tag{4}$$

The Knoop hardness (HK) number was calculated using the equation:

$$HK = \frac{14.229 \cdot P}{d^2} \tag{5}$$

where P is the applied load, d is the diagonal length of the indenter impression, 1.8544 is a constant geometrical factor for diamond pyramid and 14.229 is the geometrical constant of the diamond pyramid.

The fracture toughness can be predicted by crack propagation that can be determined by measuring the length of the cracks extending from the indent impression [22]. The fracture toughness (K_{IC}) was calculated using the following equation [23]:

$$K_{IC} = 0.016 \left(\frac{E}{HV}\right)^{1/2} \left(\frac{P}{C^{3/2}}\right) \tag{6}$$

where 0.016 is an empirical fitting constant and the half crack length is represented by C. The Young's modulus (E) was calculated using the following equation:

$$E = \frac{0.45 \cdot HK}{0.1406 \frac{b}{a}} \tag{7}$$

where a and b are the longer and shorter Knoop indentation diagonals, respectively.

The flexural strength was measured by the three-point bending test according to ISO 6872 [24] with a universal strength machine (Hounsfield, H10Ks) using a crosshead speed of 0.5 mm/min. The fracture strength (σ) of the samples was obtained using the following relation:

$$\sigma = \frac{3P \cdot l}{2w \cdot b^2} \tag{8}$$

where P is the breaking load, while the width (4 mm) and the thickness (3 mm) of the samples, and the test span (30 mm) are represented by w, b and l, respectively.

The chemical solubility (CS) of the glass-ceramic samples was investigated by following the ISO 6872 [24] standard test method. The samples were washed, dried and weighed before and after immersion in 4 vol.% acetic acid solution at 80 °C for 16 h. The CS was calculated according to the following relation:

$$CS = \frac{m_1 - m_2}{A} \tag{9}$$

where m_1 and m_2 represent the mass of the samples before and after acid leaching, respectively, and A represents a cross-sectional surface area.

III. Results and discussion

The DTA result was used as a guide for determining the sintering condition applied to induce crystallization. Figure 1 shows the DTA curve of the LD glass powder with a heating rate of 10 °C/min. The T_g was estimated to be 465 °C from the point of intersection of the tangents drawn at the slope change [25]. The two exothermic peaks at 626 and 800 °C were observed, which could be related to the first crystallization temperature (T_{C1}) and the second crystallization temperature (T_{C2}) of the glass. T_{C1} was attributed to the precipitation temperature of the lithium metasilicate (LM) phase, while T_{C2} was the transition temperature from the LM phase to the LD phase [26–29]. Therefore, the green body was sintered at 800 °C according to the crystallization temperature of the LD phase at T_{C2}. Finally, the endother-

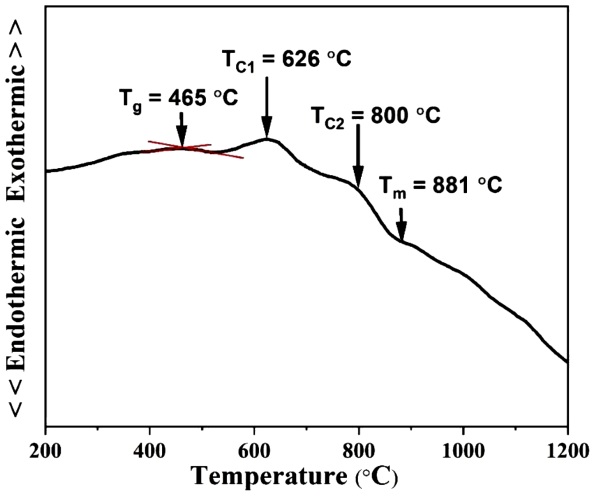

Figure 1. DTA curve of the LD glass powder

Figure 2. Appearance of the LD glass-ceramic samples with the powder-to-binder ratio of: a) 60:40, b) 55:45, c) 50:50, and d) 45:55 (vol.%) before and after sintering at 800 °C for 2 h

mic peak at 881 °C was observed as T_m of the glass. Figure 2 shows the appearance of the LD glass-ceramic samples, mixed with glass powders with various glass-to-binder ratios before and after sintering at 800 °C for 2 h. Before sintering, the samples have a whitish colour and after sintering samples have shrunk and changed in colour. The shrinkage results are shown in Table 1.

XRD patterns of the LD glass-ceramic samples after sintering at 626 and 800 °C for 2 h are shown in Fig. 3. They reveal the presence of only one prominent crystalline phase of LM (Li_2SiO_3 - JCPDS No. 29-0829) after sintering at 626 °C, while after sintering at 800 °C, LD ($Li_2Si_2O_5$ - JCPDS No. 40-0376) was detected. This result was used to confirm the crystallization temperature from the DTA result where the T_{C1} and T_{C2} were attributed to the LM phase's precipitation temperature and the transition temperature from the LM phase to the LD phase, respectively.

Microstructures of the LD glass-ceramic samples after sintering at 626 and 800 °C for 2 h are shown in Fig. 4. It was found that the sample sintered at 626 °C (Fig. 4a) has uniform spherical like structures which could be ascribed to the LM phase. This is consistent with the previous XRD analysis. Also, this is consistent with the report done by Lien *et al.* [30] and Sun *et al.* [31]. For the sample sintered at 800 °C (Fig. 4b), the image shows the rod-like shapes of the LD phase corresponding to the XRD results.

SEM images of the fracture surfaces of the LD glass-ceramic samples with various compositions after sintering at 800 °C for 2 h are shown in Fig. 5. These surfaces were not been polished and acid-etched as the pores not generated by the etching process can be clearly observed. As expected, the noticeable amount of pores can be revealed. This result is consistent with the bulk porosity values tabulated in Table 1 with the maximum value of about 3.5% as measured from the LD glass-ceramic samples with the lowest glass-to-binder ratio of 45:55 vol.% (Fig. 5d). These pores possibly occur from the removal of the binder during sintering.

Table 1 shows the bulk density, linear shrinkage and porosity of the LD glass-ceramic samples after sintering at 800 °C for 2 h. The results indicate that the bulk density values tend to decrease with decreasing glass-to-binder ratio. The LD glass-ceramic samples with glass-to-binder ratio of 60:40 and 45:55 vol.% have the highest and the lowest bulk density of 2.55 ± 0.13 and 2.35 ± 0.19 g/cm^3, respectively. The bulk density of all

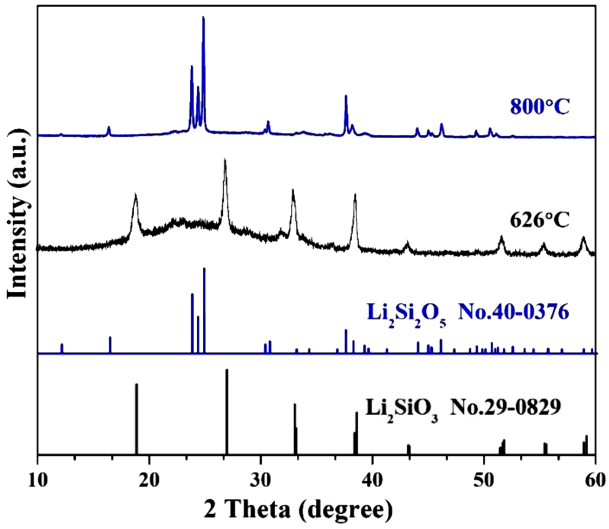

Figure 3. XRD patterns of the LD glass-ceramic samples after sintering at 626 and 800 °C for 2 h

Table 1. Bulk density, linear shrinkage and porosity of the LD glass-ceramic samples

Glass-to-binder ratio [vol.%]	Bulk density [g/cm^3]	Linear shrinkage [%]	Bulk porosity [%]
60:40	2.55 ± 0.13	16.90 ± 0.37	1.18 ± 0.11
55:45	2.50 ± 0.09	17.25 ± 0.68	1.78 ± 0.13
50:50	2.42 ± 0.16	17.98 ± 0.11	2.38 ± 0.16
45:55	2.35 ± 0.19	18.64 ± 3.25	3.55 ± 0.20

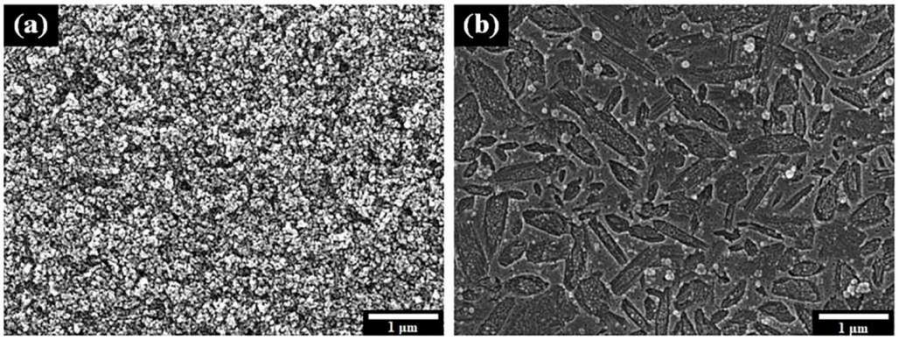

Figure 4. SEM images of the etched surfaces of the LD glass-ceramic samples after sintering at: a) 626 and b) 800 °C for 2 h

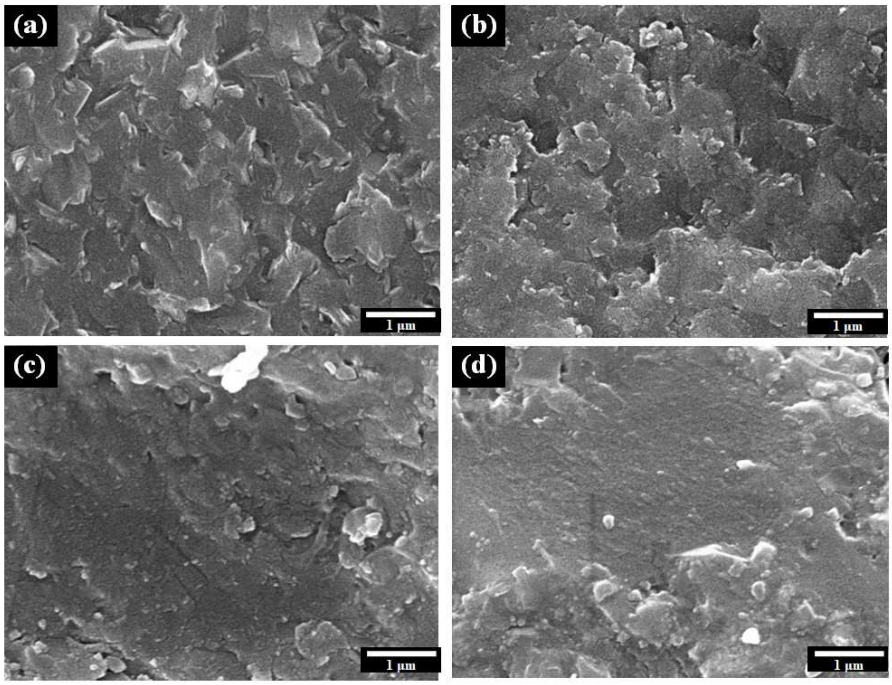

Figure 5. SEM images of fracture surfaces of the LD glass-ceramic samples with the ratio of glass powder-to-binder: a) 60:40, b) 55:45, c) 50:50 and d) 45:55 (vol.%) after sintering at 800 °C for 2 h

prepared glass-ceramic samples was close to the density of natural teeth (~2.5 g/cm^3) [32]. In contrast, the linear shrinkage and porosity of the samples tended to increase with the reduction of glass-to-binder ratio. The lowest glass powder concentration of 45 vol.% gave rise to the highest linear shrinkage and porosity, corresponding to the microstructure results.

Table 2 shows the Vickers hardness (HV), Knoop hardness (HK), Young's modulus (E), fracture toughness (K_{IC}), flexural strength (σ) and chemical solubility (CS) of the samples after sintering at 800 °C for 2 h. Ten indentations were used to evaluate the standard deviation of the mean values for the errors in measured hardness and crack lengths. Five samples per group were used to investigate the flexural strength and chemical solubility. The HV, HK, E, K_{IC} and σ results were used to analyse the mechanical properties of the samples. Ordinarily, the mechanical properties of the LD glass-ceramics depend on the microstructure and the porosity [33,34]. Especially the volume fraction of elongated micron-sized LD crystals and some minor phases, which form an interlocking network embedded into a residual glass, is crucially important in controlling the mechanical properties of this LD glass-ceramics [3]. The higher ratio of this interlocking network in a residual glass is better mechanical property of the materials can be achieved. It can be seen that there is a tendency of all values of mechanical properties (Table 3) to reduce with a decrease of glass-to-binder ratio. These results correspond to the previous results of the microstructure and porosity. All values of the mechanical properties had the maximum and minimum for the samples with glass-to-binder ratio of 60:40 and 45:55 vol.%, respectively. For the HV and HK values, regardless of the fact that these two methods had distinctively different values of hardness, there are quite similar trends in values with increasing glass-to-binder ratio. The HV values of all prepared glass-ceramic samples were found to be higher than the HV (~5.8 GPa) of the LD glass-ceramics necessary for dental applications [35].

Table 2. The mechanical properties and chemical solubility of the LD glass-ceramic samples

Glass-to-binder ratio [vol.%]	HV [GPa]	HK [GPa]	E [GPa]	K_{IC} [MPa·m$^{1/2}$]	σ [MPa]	CS [μg/cm^2]
60:40	6.80 ± 0.65	5.78 ± 0.53	66 ± 5	2.28 ± 0.17	176 ± 8	13 ± 3
55:45	6.66 ± 0.73	5.48 ± 0.41	58 ± 3	2.22 ± 0.32	137 ± 5	17 ± 4
50:50	6.39 ± 0.94	5.29 ± 0.49	47 ± 2	2.20 ± 0.43	127 ± 9	21 ± 6
45:55	6.23 ± 0.89	4.81 ± 0.62	38 ± 4	1.90 ± 0.51	91 ± 7	27 ± 5

Table 3. Comparison of the mechanical properties of the commercially available glass-ceramics and other studies with the optimum glass-ceramics in this study

Material	Manufacturing Technique	HV [GPa]	σ [MPa]
Mica-based [36,37]	Castable CAD/CAM	4–6.5	90–130
Leucite-based [38]	Hot press CAD/CAM	6.5	80–120
Lithium disilicate [39]	Hot press CAD/CAM	4–6.5	350–450
Lithium disilicate [15]	Uniaxial pressing	5.27–5.34	165–201
This study	Injection molding (optimal conditions)	6.80 ± 0.65	176 ± 8

Table 3 shows the comparison of the Vickers' hardness (HV) and flexural strength (σ) values of the commercially available glass-ceramics and other studies with the optimum glass-ceramics in this study. It is obvious that the differences in manufacturing techniques provide different values of the HV and σ. Moreover, it can be noted that our HV value from the optimum composition (glass-to-binder ratio = 60:40) is comparable with that of commercially available mica-based, leucite-based and lithium disilicate based glass ceramics made by casting and hot press CAD/CAM techniques and higher than that from uniaxial pressing technique. Although our σ value is quite low compared to that from lithium disilicate made by hot press CAD/CAM method, it is higher than that for the commercial mica-based and leucite-based glass-ceramics. This implies that our lithium disilicate glass-ceramics with optimum composition can be one of the potential candidates for alternative dental restoration materials. Additionally, the injection moulding method has been used in many of dental material industries worldwide due to its ability to form a complex shape of a dental component, overcoming the simple uniaxial technique which has limitation in forming such a complex-shape object.

The CS values are mostly dependent on the crystalline phase, microstructure, and amounts of crystals in the glassy matrix [40]. It was found that the CS increased with decreasing glass-to-binder ratio corresponding to the microstructure results. The flexural strength and chemical solubility results indicated that the prepared glass-ceramic samples could be used for fixed prostheses in the second class, according to ISO 6872 [24].

IV. Conclusions

In this study, the effects of glass-to-binder ratio on the microstructures, mechanical properties and chemical solubility of LD glass-ceramic samples were studied. The LD glass-ceramic samples were prepared by low-pressure injection moulding using the PEG-based binder. According to the differential thermal analysis result, the optimum sintering temperature of 800 °C could induce crystallization of the LD phase. Even though the addition of PEG-based binder causes negative effect on the bulk density, linear shrinkage and porosity, in this study the optimal glass-to-binder ratio of 60:40 gives the glass-ceramics with acceptable mechanical properties compared to those of the commercially available glass-ceramics and mentioned in the other studies. The highest value of the bulk density, Vickers hardness, fracture toughness and flexural strength could be obtained as 2.55 g/cm^3, 6.80 GPa, 2.28 MPa·m$^{1/2}$ and 176 MPa, respectively. Further development of this LD glass-ceramics based on the results from this study should be carried out for alternative dental restorative materials.

Acknowledgements: This work is financially supported by the Royal Golden Jubilee Ph.D. Program, the National Research Council of Thailand, the Materials Science Research Center, the Department of Physics and Materials, Faculty of Science, and the Graduate School Chiang Mai University, Thailand.

References

1. M. Laczka, K. Laczka, K. Cholewa-Kowalska, A.B. Kounga, C. Appert, "Mechanical properties of a lithium disilicate strengthened lithium aluminosilicate glass-ceramic", *J. Am. Ceram. Soc.*, **97** [2] (2014) 361–364.
2. Z. Peng, M.I.A. Rahman, Y. Zhang, L. Yin, "Wear behavior of pressable lithium disilicate glass ceramic", *J. Biomed. Mater. Res. B. Appl. Biomater.*, **104** (2016) 968–978.
3. M.O.C. Villas-Boas, F.C. Serbena, V.O. Soares, I. Mathias, E.D. Zanotto, "Residual stress effect on the fracture toughness of lithium disilicate glass-ceramics", *J. Am. Ceram. Soc.*, **103** (2020) 465–479.
4. H. Zhang, Z. He, Y. Zhang, W. Jing, B. Wang, J. Yang, "Lithium disilicate glass-ceramics by heat treatment of lithium metasilicate glass-ceramics obtained by hot pressing", *J. Am. Ceram. Soc.*, **98** [12] (2015) 3659–3662.
5. F. Wang, Z. Chai, Z. Deng, J. Gao, H. Wang, J. Chen, "Effect of heat-pressing temperature and holding time on the microstructure and flexural strength of lithium disilicate

glass-ceramics", *PLoS One*, **10** (2015) e0126896.
6. A.X. Lu, Z.B. Ke, Z.H. Xiao, X.F. Zhang, X.Y. Li, "Effect of heat-treatment condition on crystallization behavior and thermal expansion coefficient of Li_2O-ZnO-Al_2O_3-SiO_2-P_2O_5 glass-ceramics", *J. Non-Cryst. Solids*, **353** [28] (2007) 2692–2697.
7. S.E. Elsaka, A.M. Elnaghy, "Mechanical properties of zirconia reinforced lithium silicate glass-ceramic", *Dent. Mater.*, **32** [7] (2016) 908–914.
8. S. Huang, P. Caon, C. Wang, Z. Huang, W. Gao, "Fabrication of a high-strength lithium disilicate glass-ceramic in a complex glass system", *J. Asian Ceram. Soc.*, **1** (2013) 46–52.
9. E. El-Meliegy, R.V. Noort, *Glasses and Glass Ceramics for Medical Applications*, Springer, New York 2012.
10. H.R. Fernandes, D.U. Tulyaganov, J.M.F. Ferreira, "The role of P_2O_5, TiO_2 and ZrO_2 as nucleating agents on microstructure and crystallization behaviour of lithium disilicate-based glass", *J. Mater. Sci.*, **48** (2013) 765–773.
11. X. Zheng, G. Wen, L. Song, X.X. Huang, "Effects of P_2O_5 and heat treatment on crystallization and microstructure in lithium disilicate glass ceramics", *Acta. Mater.*, **56** [3] (2008) 549–558.
12. F. Wang, J. Gao, H. Wang, J. Chen, "Flexural strength and translucent characteristics of lithium disilicate glass-ceramics with different P_2O_5 content", *Mater. Des.*, **31** [7] (2010) 3270–3274.
13. H.R. Fernandes, D.U. Tulyaganov, A. Goel, M.J. Ribeiro, M.J. Pascual, J.M.F. Ferreira, "Effect of Al_2O_3 and K_2O content on structure, properties and devitrification of glasses in the Li_2O-SiO_2 system", *J. Eur. Ceram. Soc.*, **30** [10] (2010) 2017–2030.
14. S.C.V. Clausbruch, M. Schweiger, W. Höland, V. Rheinberger, "The effect of P_2O_5 on the crystallization and microstructure of glass-ceramics in the SiO_2-Li_2O-K_2O-ZnO-P_2O_5 system", *J. Non-Cryst. Solids*, **263-264** (2000) 388–394.
15. D.U. Thlyaganov, S. Agathopoulos, I. Kansal, P. Valerio, "Synthesis and properties of lithium disilicate glass-ceramics in the system SiO_2-Al_2O_3-K_2O-Li_2O", *Ceram. Int.*, **35** [8] (2009) 3013–3019.
16. L. Gorjan, A. Dakskobler, T. Kosmac, "Partial wick-debinding of low-pressure powder injection-moulded ceramic parts", *J. Eur. Ceram. Soc.*, **30** [15] (2010) 3013–3021.
17. M. Sardarian, O. Mirzaee, A. Habibolahzadeh, "Influence of injection temperature and pressure on the properties of alumina parts fabricated by low pressure injection molding (LPIM)", *Ceram. Int.*, **43** [6] (2017) 4785–4793.
18. G. Thavanayagam, D.L. Zhang, K.L. Pickering, S. Rayanova, "A study of polyvinyl butyryl based binder system in titanium based metal Injection moulding", *Key Eng. Mater.*, **520** (2012) 167–173.
19. Y. Thomas, B.R. Marple, "Partially water-soluble binder formulation for injection molding submicrometer zirconia", *Adv. Perform. Mater.*, **5** (1998) 25–41.
20. Y. Gao, K. Huang, Z. Fan, Z. Xie, "Injection molding of zirconia ceramics using water-soluble binders", *Key Eng. Mater.*, **336-338** (2007) 1017–1020.
21. D.B. Marshall, T. Noma, A.G. Evans, "A simple method for determining elastic-modulus-to-hardness ratios using Knoop indentation measurements", *J. Am. Ceram. Soc.*, **65** (1982) c175–c176.
22. G.R. Anstis, P. Chantikul, B.R. Lawn, D.B. Marshall, "A critical evaluation of indentation techniques for measuring fracture toughness: I, direct crack measurements", *J. Am. Ceram. Soc.*, **64** [9] (1981) 533–538.
23. M.A. Zoroddu, J. Aashet, G. Crisponi, S. Medici, M. Peana, V.M. Nurchi, "The essential metals for humans: A brief overview", *J. Inorg. Biochem.*, **195** (2019) 120–129.
24. ISO 6872: 2015 (E), *Dentistry - Ceramic Materials*, fourth edition, International Standards Organization.
25. M. Kamnoy, W. Leenakul, P. Intawin, U. Intatha, S. Eittsayeam, "Effect of heat treatment temperature on the microstructure and mechanical properties of Li_2O-SiO_2-P_2O_5-Al_2O_3-K_2O-CaO glass-ceramics", *Sci. Adv. Mater.*, **10** [9] (2018) 1–5.
26. A. Gaddam, H.R. Fernandes, M.J. Pascual, "Influence of Al_2O_3 and B_2O_3 on sintering and crystallization of lithium silicate glass system", *J. Am. Ceram. Soc.*, **99** [3] (2016) 833–840.
27. S. Kolay, P. Bhargava, "Phase and microstructural evolution in lithium silicate glass-ceramics with externally added nucleating agent", *J. Am. Ceram. Soc.*, **102** (2019) 7312–7328.
28. G. Wen, X. Zheng, L. Song, "Effects of P_2O_5 and sintering temperature on microstructure and mechanical properties of lithium disilicate glass-ceramics", *Acta Mater.*, **55** [10] (2007) 3583–3591.
29. T. Zhao, A.J. Li, Y. Qin, J.F. Zhu, X.G. Kong, J.F. Yang, "Influence of SiO_2 contents on the microstructure and mechanical properties of lithium disilicate glass-ceramics by reaction sintering", *J. Non-Cryst. Solids*, **512** (2019) 148–154.
30. W. Lien, H.W. Roberts, J.A. Platt, K.S. Vandewalle, T.J. Hill, T.G. Chu, "Microstructural evolution and physical behavior of a lithium disilicate glass-ceramic", *Dent. Mater.*, **31** [8] (2015) 928–940.
31. Y. Sun, L. Ma, P. Wang, Z. Ke, Z. Zhang, Y. Yang, J. Wang, Q. Sun, L. Feng, T. Wang, "Effects of heat treatment on the crystallization behavior, microstructure and thermal properties of a complex Li_2O-SiO_2 glass system", *Ceram. Int.*, **46** [10] (2020) 15113–15121.
32. R.A. Farah, M.V. Swain, B.K. Drummond, R. Cook, M. Atieh, "Mineral density of hypomineralised enamel", *J. Dent.*, **38** [1] (2010) 50–58.
33. D. Li, J.W. Guo, X.S. Wang, S.F. Zhang, L. He, "Effects of crystal size on the mechanical properties of a lithium disilicate glass-ceramic", *Mater. Sci. Eng. A*, **669** (2016) 332–339.
34. L. Hallmann, P. Ulmer, M. Kern, "Effect of microstructure on the mechanical properties of lithium silicate glass-ceramics", *J. Mech. Behav. Biomed. Mater.*, **82** (2018) 355–370.
35. J.L. Fu, H. Engqvist, W. Xia, "Glass-ceramics in dentistry: A review", *Materials*, **13** [5] (2020) 1049.
36. I.L. Denry, J.A. Holloway, "Effect of heat pressing on the mechanical properties of a mica-based glass-ceramic", *J. Biomed. Mater. Res. Part B Appl. Biomater.*, **70** (2004) 37–42.
37. S. Gali, "Mica glass ceramics for dental restorations", *Mater. Technol.*, **34** [1] (2019) 2–11.
38. X. Chen, T.C. Chadwick, R.M. Wilson, R.G. Hill, M.J. Cattell, "Crystallization and flexural strength optimization of fine-grained leucite glass-ceramics for dentistry", *Dent. Mater.*, **27** [11] (2011) 1153–1161.

39. F. Zarone, M.I. Di Mauro, P. Ausiello, G. Ruggiero, R. Sorrentino, "Current status on lithium disilicate and zirconia: a narrative review", *BMC Oral Health*, **19** [1] (2019) 134.

40. S.M. Salman, S.N. Salama, H.A. Abo-Mosallam, "Crystallization features and physicochemical properties of alkali and alkaline aluminoborate glass-ceramics", *J. Austral. Ceram. Soc.*, **53** (2017) 953–961.